11th International Conference "Environmental Engineering"
Vilnius Gediminas Technical University
Lithuania, 21–22 May 2020
Section: Smart Cities, Roads and Railways
http://enviro.vgtu.lt

eISSN 2029-7092 / eISBN 978-609-476-232-1

Article ID: enviro.2020.623
https://doi.org/10.3846/enviro.2020.623

The Study of Road Pavement Performance Through Impact Hammer Tests

Filippo G. Praticò, Gianfranco Pellicano*, Rosario Fedele

Department of Information Engineering, Infrastructure, and Sustainable Energy (D IIES), University Mediterranea of Reggio Calabria, Italy

Received 05 February 2020; accepted 20 April 2020

Abstract. Noise pollution has become an important issue. One of the main sources of noise in residential areas is represented by transportation and by the interaction between tyre and road surface. Several studies illustrate that traffic noise is affected by road properties such as acoustic absorption, surface texture, and mechanical impedance. This latter, function of the angular frequency ω, is defined as the ratio of a force applied on a structure to the induced velocity. Despite a growing interest in mechanical impedance there is still lack of results about its impact on traffic noise. Consequently, the aim of the study presented in this paper is to investigate the relationship between road acoustic response and mechanical impedance. Tests (EN 29052-part 1, ISO 7626-5) have been performed on different types of samples and materials, using an impact hammer and an accelerometer. Investigations are still in progress. First results seem to demonstrate that both frequencies and other noise-related characteristics could be affected by changes of mechanical impedance, boundary conditions, tests, and type of material.

Keywords: mechanical impedance, road reliability, impact hammer test, traffic noise, acoustical response, dynamic stiffness.

Introduction

According to the World Health Organization (WHO), the health impacts of environmental noise are a growing concern among both the general public and policy-makers in Europe (WHO Europe, 2011).

With conservative assumptions applied to the calculation methods, at least one million healthy life years are lost every year from traffic-related noise in the western part of Europe. For this reason, one of the most important road requirement is to include a low noise contribution (Praticò, 2011). Traffic produces noise and vibrations that generate a negative impact on the livability, the performance, and the durability of the built environment that surrounds and includes transportation infrastructures (Praticò, 2014; Praticò et al., 2019; Merenda et al., 2019; Fedele et al., 2018). Note that tyre noise depends on its structural health status where its wear at the interface influences the life and cycle costs of pavements and is a source of environmental harm (Praticò et al., 2010).

Generation mechanisms of tyre/pavement noise can be divided into two main groups: one group is related to the vibration of tyre including the tread impact and adhesion, the other group is related to the aerodynamic effect (Sandberg & Ejsmont, 2002). The vibrations generated from rolling tyre are dependent on tyre tread design, macrotexture in the road surface, and friction between tyre and road surface. In addition, another parameter that has gained importance over time and that can influence the level of vibration is represented by the mechanical impedance (Keulen & Duškov, 2005). This latter is defined, at a given point in a vibratory system, as the ratio of a sinusoidal force applied to the system at that point to the velocity at the same point (Harris & Piersol, 2002).

Some authors studied the relationship between mechanical impedance and the acoustic response. Li et al. (2012, 2016) made laboratory and in-situ measurements for investigating the mechanical impedance on different types of road surface. The investigation interested thin layer surfaces used to reduce noise on urban roads in The Netherlands, combining the advantages of Stone Mastic Asphalts (SMAs) and porous asphalts. In the project PERSUADE (Bendtsen et al., 2013; Skov et al., 2015), drainability, absorption, texture as well as mechanical impedance were measured and used as indicators for the acoustical properties of the surfaces. Different slabs of Poroelastic Road Surfacing (PERS) consisting in a mix of stone and rubber from scrapped tyres, were tested.

*Corresponding author. E-mail: *gia.pellicano@gmail.com*

Despite a growing interest in mechanical impedance and similar response functions there is still lack of results about its impact on traffic noise. Consequently, the aim of the study presented in this paper is to investigate the relationship between road acoustic response and response functions (namely, mechanical impedance).

Based on the literature review and in order to study the relationship between acoustic response and mechanical impedance, the following tasks were carried out:

Task 1: Analysis of literature and standards.

Task 2: Set up of the methodology.

Task 3: Design of experiments and experiments.

Task 4: Results analysis.

1. Task 1. Analysis of literature and standards

A Frequency Response Function (FRF, e.g., dynamic stiffness and mechanical impedance) gives insights into a structure's resonant frequencies (e.g., peaks or dips), damping (width of the peaks), and mode shapes (Siemens, 2019). Many types of input excitations and response outputs can be used to calculate an experimental FRF: 1) For mechanical systems, inputs in force (Newtons, N) and outputs in Acceleration (g's), Velocity (m/s) or Displacement (meter, m). 2) For acoustical systems, inputs in Q (Volume Acceleration, m^3/s^2) and outputs in Sound Pressure (Pascals, Pa). 3) For combined acoustic and mechanical systems, inputs in force (either Q or Newtons) and outputs in Sound Pressure (Pa), Acceleration (g's). 3) For rotational mechanical systems, inputs in Torque (Nm) and output in Rotational Displacement (degrees). For an experimental modal analysis on a mechanical structure, typically the input is a force and output is an acceleration, velocity or displacement. There are different formats that can be used for FRF, based on the math operations on the FRF: 1) integration and differentiation (acceleration can be changed to velocity or displacement); 2) inversion (the FRF can be inverted, so it is input over output, rather than output over input). Note that, in the frequency domain, integration and differentiation correspond to division and multiplication by jω, respectively, where ω is the frequency in radians per second and j is the imaginary number (Siemens, 2019). Among the standards that refer to FRFs the following can be listed: USAS S2.6 (1963), EN 29052-1 (1992), ISO 7626-5 (2019), ASTM C125 (2002), EN 14146 (2004) (Bede & Kožar, 2016).

2. Methods to derive dynamic stiffness

As is well known, while the modulus (ratio of stress to strain) is an intrinsic property of materials, the stiffness (basically referred to the ratio of force or stress to displacement) depends on geometry. The standard EN 29052-1 (1992) allows determining the dynamic stiffness of materials used under floating floors in dwellings. In this case, the dynamic stiffness is defined as the ratio of stress to displacement (MPa/m):

$$S = \frac{(F / S)}{\Delta d}, \tag{1}$$

where: F is the dynamic force applied perpendicularly to the sample, S is the surface of the sample, Δd is the dynamic variation of sample thickness. Several authors applied the above-mentioned standard to asphalt concrete specimens. For instance, Vázquez and Paje (2012) applied the standard mentioned above to test samples consisting in four different SMA mixtures to derive the apparent stiffness, and compared these results with the *stiffness modulus* (again, ratio of stress to strain) calculated applying the EN 12697-26 (indirect tensile test, MPa, (EN 12697-26 2004)) (see Table 1). In contrast, the apparent stiffness s'_t (MPa/m) was calculated using the following expression:

$$s'_t = 4\pi^2 m'_t (fr)^2, \tag{2}$$

where m'_t is the load mass per unit area (kg/m^2), and f_r is the resonant frequency (Hz) of the fundamental vibration system constituted by the load plate (which acts as a mass, with a mass per unit area of 200 kg/m^2 according to (EN 29052-1 1992)), and the sample (which acts as a spring).

In another work, Vázquez and Paje (2015) calculated the dynamic stiffness (MN/m, non-resonant method) of SMA samples using Hot, Warm, and Cold Mix Asphalt blending (i.e., HMA, WMA, and CMA, respectively), by means of a vibration exciter (source) and of an impedance head (receiver, see Table 1).

Table 1. Dynamic stiffness of different types of materials

Parameter	Material	Value	Reference
Dynamic Stiffness (Resonant method, RM, EN 29052-1)	SMA with rubber modified bitumen (max aggregate size 16 mm)	About 260 MPa/m	(Vázquez & Paje, 2012)
Dynamic Stiffness (RM, EN 29052-1)	SMA with (a) max aggregate size 16 mm and (b) max aggregate size 11 mm	About 355 MPa/m (a), and about 190 MPa (b)	
Dynamic Stiffness (RM, EN 29052-1)	SMA with polymer modified bitumen (max aggregate size 11 mm)	About 215 MPa/m	
Stiffness modulus (EN 12697-26)	SMAs above	2515-5162 MPa	
Dynamic stiffness at 400 Hz (non-resonant method)	SMA-HMA	About 23 MN/m	(Vázquez & Paje, 2015)
Dynamic stiffness at 400 Hz (non-resonant method)	SMA-WMA	About 17 MN/m	
Dynamic stiffness at 400 Hz (non-resonant method)	SMA-CMA	About 12 MN/m	
Dynamic stiffness at 400 Hz (non-resonant method)	SMA-HMA with (a) 10% of RAP and (b) 20% of RAP	About 24 MN/m (a), and about 25 MN/m (b)	

3. Methods to derive mechanical impedance

The mechanical impedance is a measure of how much a structure resists motion (e.g., speed) when subjected to a unit force. The most direct technique to determine mechanical impedance is to utilize force and motion measuring transducers (Radenberg et al., 2017). By definition, the mechanical impedance *Z*, at a given point in a vibratory system, is the ratio of a sinusoidal driving force F acting on the system to the resulting velocity v of the system (Harris & Pierol, 2002):

$$F = F_0 e^{j\omega t}; \tag{3}$$

$$v = v_0 e^{j(\omega t+\varphi)}, \tag{4}$$

where: F_0 is the magnitude of force F (N); v_0 is the magnitude of velocity v (m/s); ω is the angular frequency (Hz); ϕ is the phase angle between F and v (degrees). So, the mechanical impedance of the system *Z* (at the point of application of the force) is given by:

$$Z = F/v. \tag{5}$$

Morcillo et al. (2019) carried out tests on three different specimens, using a mechanical impedance setup that consisted of an impact hammer and an impedancimeter, and derived the Equivalent Young's Modulus. The authors defined the mechanical impedance of the road $Z_{road}(\omega)$ as:

$$Z_{road}(\omega) = Z(\omega) - i\omega m_i = \frac{F(\omega)}{V(\omega)} - i\omega m_i, \tag{6}$$

where: ω is the angular frequency (=$2\pi f$), $Z(\omega)$ is the mechanical impedance measured by the impedance meter (Ns/m), *i* is the imaginary unit, m_i is the mass of the impedance meter, $F(\omega)$ and $V(\omega)$ are the Force (N) and the Velocity (m/s) measured by the impact hammer and the impedancimeter, respectively.

Li et al. (2016) carried out tests on slabs and trial sections (air voids content in the range 8–12%, and >20% by volume) using an impact hammer and three accelerometers, in order to derive the indicator MI' (dB, re 1 Ns/m) from the amplitudes of force and velocity (in the time domain), using the expression:

$$MI' = \frac{MaxForce}{MaxVelocity}. \tag{7}$$

The results show that the indicator MI' was about 48 dB for nine HMA slabs, about 37 dB for a poroelastic surface, about 58 dB for a cement concrete surface, and about 53 dB for the six trial sections. Finally, the relation between the mechanical impedance (expressed in terms of MI'), and the resilient modulus at 500 Hz (from the master curves) was derived applying the cyclic Indirect Tension Tests (ITT) on 5 cores (extracted from 2 slabs and 3 trial sections cited above), and using the Universal Testing Machine (UTM). The results showed that the mechanical impedance is linearly related to the logarithm of the resilient modulus.

4. Task 2 and 3. Set up of the methodology, design of experiments, and experiments

In this study, laboratory tests were carried out on different types of materials, using an impact hammer, an accelerometer, and a microphone. The equipment used for tests was composed by an impact hammer "Brüel & Kjaer Type 8206" to register the applied force (that does not apply additional mass loading), a piezoelectric accelerometer "Brüel & Kjaer Type 4507" with a frequency range of 0.3÷6000 Hz, an omnidirectional pre-polarized microphone "Audix TM1" (Frequency Response = 20 Hz÷25 kHz +/–2 dB, Sensitivity = 6 mV/Pa @ 1 kHz, Dynamic Range = 112 dB) with an external audio card "Roland quad-capture UA-55" in order to obtain sound pressure generated from each hammer hit. Instrumentation was connected to a system consisting of a laptop computer and a Brüel & Kjaer front-end acquisition board, which was used to convert (using the Fast Fourier Transform, FFT) the hammer's time series to frequency responses. Ten hits were applied for each impact hammer test, while a set of signals over time were recorded using a sampling rate of 3.2 kHz. In case of slabs, the hitting point was chosen in the middle of the upper surface while the accelerometer was fixed on a steel sheet with dimensions 40×20 mm, glued with bitumen at 20 mm from the hitting point (cf. a_1 and a_2 in Figure 1).

The flow chart in Figure 1 illustrates the experimental procedure followed during the laboratory tests. In some measurements the sample tested was cylindrical, in some case rectangular slabs were used (Figure 1, a_3). By using the impact hammer, hits were applied on load plate or directly on the upper face of the specimen. The mechanical impedance (based on force and speed, cf. Eq. (5) and the dynamic stiffness (based on force and displacement, cf. Eq. (1) were derived (cf. Figure 1b and 1c). For each natural frequency (fn, cf. Figure 1d) of the material tested, a dynamic stiffness value (Figure 1e) was obtained (see Table 3). Due to the complexity of experiments and to the fact that many parameters affect the results, during the preliminary measurements, results were compared to a MDoF system in order to control their reasonableness. To this end it is noted that, in first approximation, each sample can be seen as a mass-spring-damper system with a Single Degree of Freedom (SDoF). However, if the test is carried out while the sample is attached on the pavement, and if a load plate is used, a system with a Multiple Degree of Freedom (MDoF) should be considered.

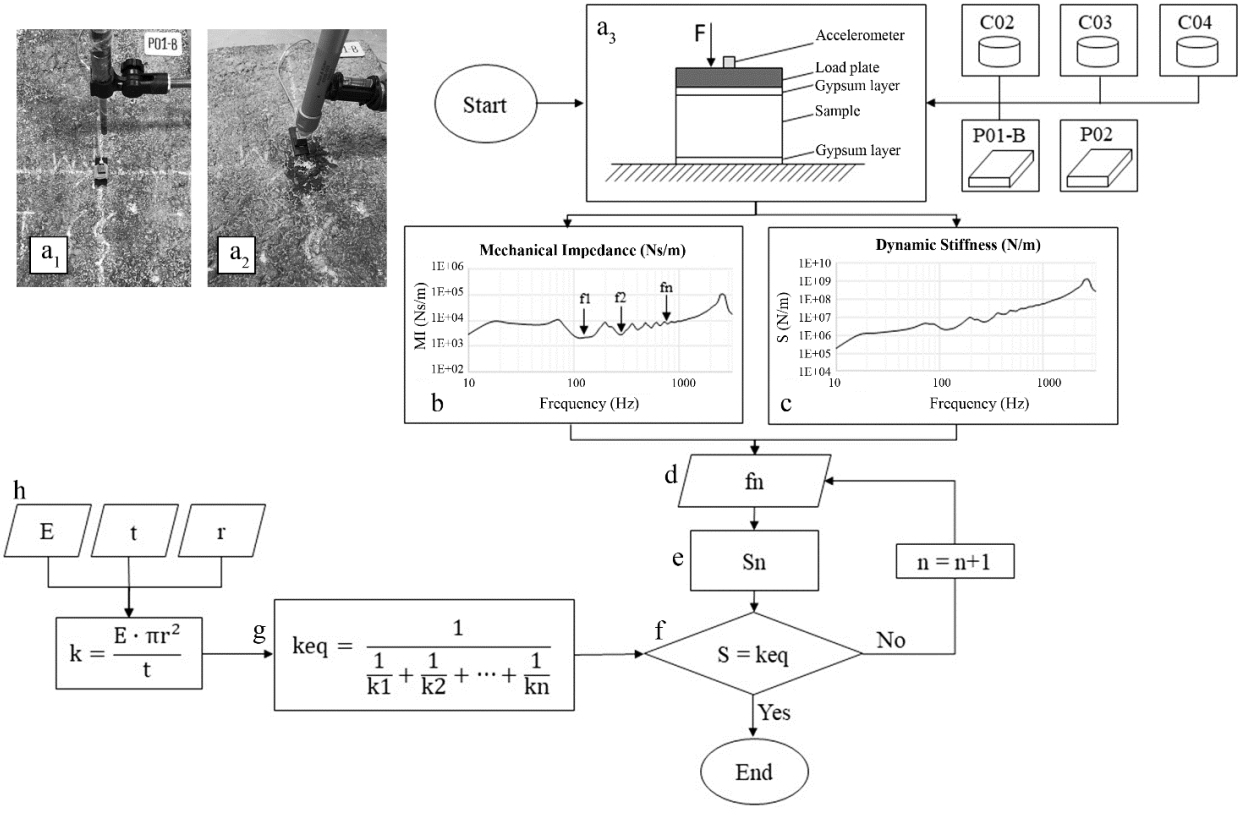

Legend. fn=natural frequency (Hz) (n=1,…N); Sn=dynamic stiffness (N/m) (n=1,…N); keq=equivalent dynamic stiffness; E=Young's modulus (MPa); t=thickness (m); r=radius (m); C02=cylindrical sample (rubber); C03=cylindrical sample (HMA open graded); C04=cylindrical sample (HMA dense graded); P01-B=slab (HMA dense graded); P02=slab (rubber).

Figure 1. Flow chart of experimental procedure (Task 2)

Consequently, the dynamic stiffness obtained through the equation 1 was compared with the one derived based on a vibration system model of springs in series, where the equivalent stiffness is given by *keq* (cf. Figure 1g). This

latter was obtained as a function of the Young's modulus, the thickness, and the radius of each body in series (Figure 1h). In turn, the moduli were assessed based on the literature and based on in lab expedite measurements. Based on Task 2, it was possible to set up the methodology and to compare it with the one reported in the standard EN 29052-1 in the pursuit of having a methodology complying with the one set up in the standard but that can be used also when different samples with different geometry are given.

In Task 2, experiments were designed. In Table 2 different types of materials and boundary conditions are presented, for each case study that was taken into account. Note that both rectangular slabs and cylindrical samples were considered, for HMA and rubber samples. For the Resonant Method, it is necessary to place a mass on the top of the studied surface (Vázquez & Paje, 2016).

Table 2. Boundary conditions for each material tested

Test	Material	Sample		Load Plate			Gypsum			Underlayer			Output
		Cylinder	Slab	⌀ 10 cm	⌀ 1 cm	None	Top/bottom	Bottom	None	Pavement	Stone	Steel	
C02_I	Rubber	x		x			x			x			k; MI; f
C02_II	Rubber	x			x			x		x			
C02_III	Rubber	x		x					x			x	
C03_I	HMA	x		x			x			x			
C03_II	HMA	x			x			x		x			
C04_I	HMA	x		x			x			x			
C04_II	HMA	x			x			x		x			
C04_III	HMA	x		x			x				x		
C04_IV	HMA	x		x					x		x		
C04_V	HMA	x		x					x	x			
C04_VI	HMA	x		x					x			X	
P02_I	Rubber		x		x				x	x			
P02_II	Rubber		x		x				x		x		
P01-B_I	HMA		x		x				x	x			
P01-B_II	HMA		x		x				x		x		
P01-B_III	HMA		x		x				x	x			
P01-B_IV	HMA		x			x			x	x			
P01-B_a	HMA		x			x			x	x			AR; k; MI; f
P01-B_b	HMA		x			x			x	x			
P01-B_c	HMA		x			x			x	x			
P02_a	Rubber		x			x			x	x			
P02_b	Rubber		x			x			x	x			
P02_c	Rubber		x			x			x	x			
P04_a	Steel		x			x			x	x			
P04_b	Steel		x			x			x	x			
P04_c	Steel		x			x			x	x			

Note. C02: rubber; C03: Hot Mix Asphalt (HMA) open graded; C04: HMA dense graded; P02: rubber; P01-B: HMA dense graded; P04: steel; C02_I: first test on the sample C02; P01-B_a: first acoustic test on the sample P01-B; k: dynamic stiffness; MI: mechanical impedance; f: natural frequencies; AR: acoustic response.

5. Task 4. Results analysis

As is well known, in a mechanical impedance Frequency Response Function (FRF), the dips correspond to the natural frequencies of the test system (Siemens, 2019). Figure 2 illustrates (a) the mechanical impedance and (b) the dynamic stiffness (cf. EN 29052-1) as a function of frequency for the cylindrical sample C02 (rubber, cf. Table 2). A natural frequency at about 32 Hz is present.

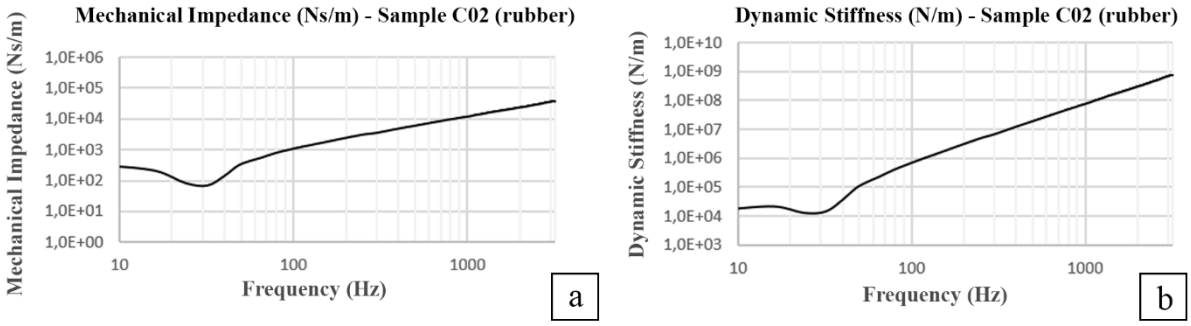

Figure 2. Mechanical impedance (a), and dynamic stiffness (b) for cylindrical sample C02 (rubber)

In the case of the HMA cylindrical sample C04, different natural frequencies are obtained (at about 120, 288, 432 and 552 Hz), as illustrated in Figure 3a. Based on Eq. (1), for each frequency a dynamic stiffness value was derived (cf. Table 3).

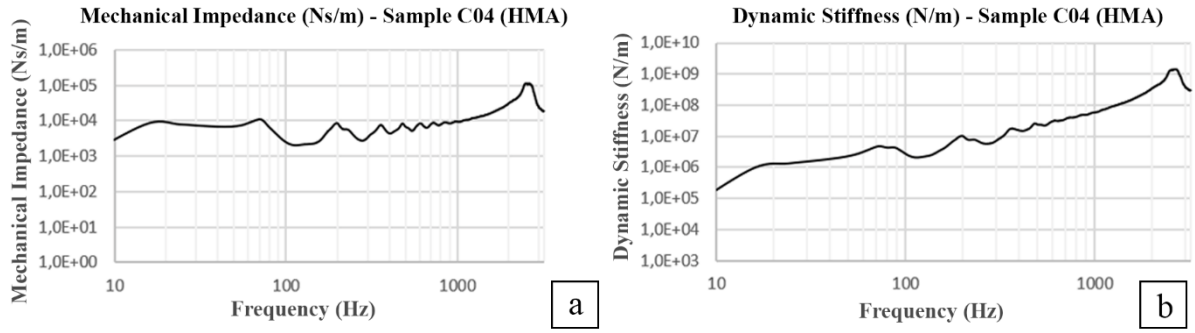

Figure 3. Mechanical impedance (a), and dynamic stiffness (b) for cylindrical sample C04 (HMA)

Figure 4 illustrates the influence of the load plate (1 cm of diameter) on the mechanical impedance, for the slab P01-B in HMA. The curves of the mechanical impedance (a) and of the dynamic stiffness (b) appear to be unaffected by the presence of the load plate, except that for the frequency range of 100÷300 Hz.

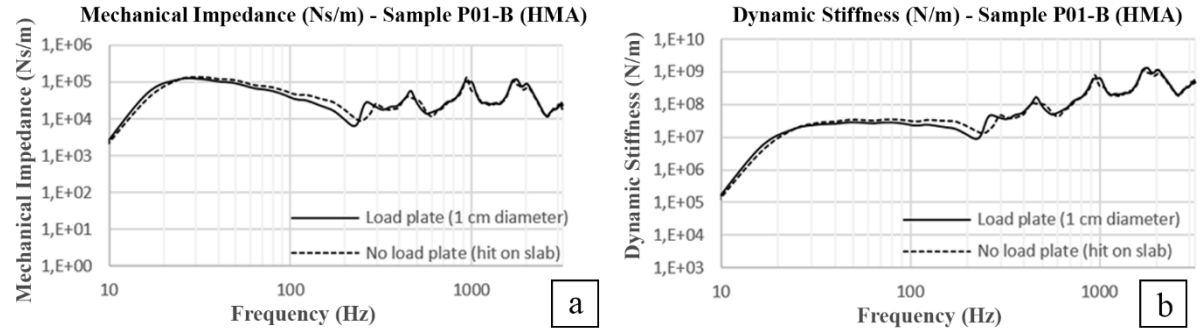

Figure 4. Mechanical impedance (a), and dynamic stiffness (b) for slab P01-B (HMA)

Figure 5 illustrates the relationship between mechanical impedance and acoustic response, for the measurement carried out on the slab P01-B placed on a pavement. In a first test, ten hammer drops were applied directly on the slab, with an average force value of 80 N (Figure 5a). In a second test the force was increased with an average value of 130 N (Figure 5b). In both cases, the mechanical impedance and acoustic response peaks appear to be translated of about 400 Hz.

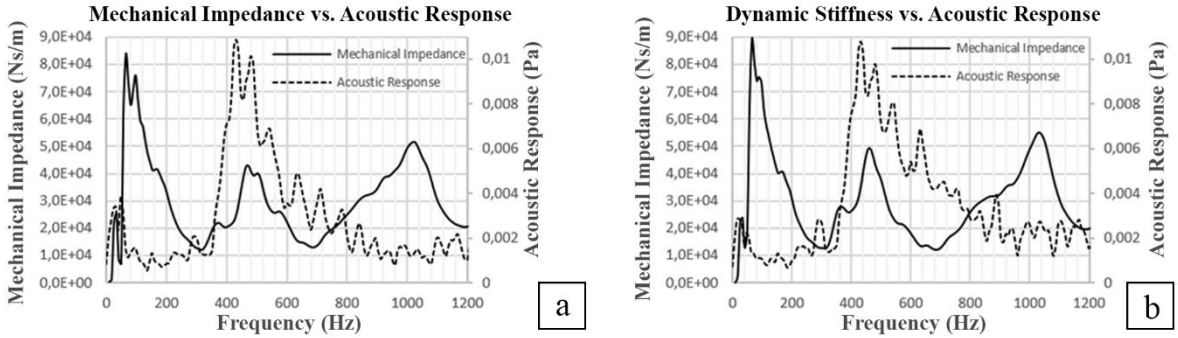

Figure 5. Relationship between mechanical impedance and acoustic response for an average force of (a) 80 N and (b) 130 N, respectively

Table 3 illustrates the natural frequencies (e.g., f_1) and the corresponding values of dynamic stiffness (e.g., $k(f_1)$). Furthermore, the equivalent stiffness (k_{eq}) defined in Figure 1 is reported. Note that f_i and $k(f_i)$ were derived based on FRF (resonant method, (Vázquez & Paje, 2016)), while k_{eq} was derived based on moduli and geometry.

Table 3. Dynamic stiffness values for each natural frequency

Test	f_1(Hz)	$k(f_1)$ (N/m)	f_2(Hz)	$k(f_2)$ (N/m)	f_3(Hz)	$k(f_3)$ (N/m)	f_4(Hz)	$k(f_4)$ (N/m)	f_5(Hz)	$k(f_5)$ (N/m)	k_{eq} (N/m)
C02_I	32	1.43E+04	–	–	–	–	–	–	–	–	1.41E+04
C02_II	128	6.38E+03	256	1.21E+04	–	–	–	–	–	–	1.41E+04
C02_III	40	1.75E+04	–	–	–	–	–	–	–	–	1.41E+04
C03_I	288	3.75E+06	456	1.04E+07	568	1.78E+07	768	2.67E+07	1032	4.94E+07	3.41E+01
C03_II	320	4.63E+07	496	8.91E+07	1248	1.34E+08	2320	9.86E+06	–	–	3.41E+01
C04_I	120	2.13E+06	288	6.13E+06	432	1.56E+07	552	2.26E+07	–	–	4.84E+01
C04_II	128	2.27E+07	304	4.06E+07	704	4.44E+07	–	–	–	–	4.84E+01
C04_III	216	2.49E+06	288	6.42E+06	344	9.90E+06	424	9.29E+06	512	1.53E+07	4.84E+01
C04_IV	144	1.19E+06	288	3.29E+06	456	8.96E+06	616	1.54E+07	–	–	4.84E+01
C04_V	232	2.38E+06	344	4.70E+06	544	1.21E+07	648	1.66E+07	–	–	4.84E+01
C04_VI	224	8.51E+06	376	9.16E+06	680	2.08E+07	808	4.83E+07	–	–	4.84E+01
P02_I	56	3.43E+04	136	1.55E+04	232	7.05E+04	288	1.73E+05	336	6.79E+04	1.26E+04
P02_II	48	1.78E+04	96	4.41E+04	128	6.30E+04	208	7.70E+04	360	1.34E+05	1.26E+04
P01-B_I	48	1.17E+07	232	8.10E+06	376	6.72E+07	576	4.18E+07	1048	1.75E+08	3.91E+07
P01-B_II	56	2.07E+07	120	1.62E+07	328	2.50E+07	624	7.21E+07	1008	1.10E+08	4.60E+07
P01-B_III	232	9.35E+06	336	3.72E+07	592	5.06E+07	1288	2.01E+08	–	–	3.91E+07
P01-B_IV	248	1.36E+07	360	4.01E+07	616	4.58E+07	1312	1.98E+08	–	–	3.91E+07

Note. C02: rubber; C03: Hot Mix Asphalt (HMA) open graded; C04: HMA dense graded; P02: rubber; P01-B: HMA; C02_I: first test on the sample C02.

Table 4 and Figure 6 refer to the first results obtained in terms of relationship between acoustic response, AR, and mechanical impedance, MI. Higher energies yield higher ARs, for a given MI. For a given hammer height (energy) higher MI (and/or moduli) correspond to higher ARs. Note that based on the analyses carried out and based on Figure 5, the best correlation between AR and MI refers to frequencies in the range 0–400 Hz.

Table 4. Mechanical impedance and acoustic response maximum values

Test	Material	Hammer height (m)	F (N)	MI max (Ns/m)	MI max (dB)	AR max (Pa)
P01-B_a	HMA	0.05	≈ 82	8.45E+04	98.5	1.41
P01-B_b	HMA	0.10	≈ 129	8.93E+04	99.0	1.98
P01-B_c	HMA	0.15	≈ 252	9.49E+04	99.5	3.74

End of Table 4

Test	Material	Hammer height (m)	F (N)	MI max (Ns/m)	MI max (dB)	AR max (Pa)
P02_a	Rubber	0.05	≈ 3	7.09E+03	77	0.01
P02_b	Rubber	0.10	≈ 8	8.33E+03	78.4	0.01
P02_c	Rubber	0.15	≈ 12	6.93E+03	76.3	0.02
P04_a	Steel	0.05	≈ 119	7.26E+05	117.2	1.85
P04_b	Steel	0.10	≈ 242	9.83E+05	119.9	3.99
P04_c	Steel	0.15	≈ 302	9.26E+05	119.3	5.17

Note. P01-B: slab Hot Mix Asphalt (HMA); P02: slab rubber; P04: slab steel; P01-B_a: first test on the sample P01-B; F: force; MI: mechanical impedance; AR: acoustic response.

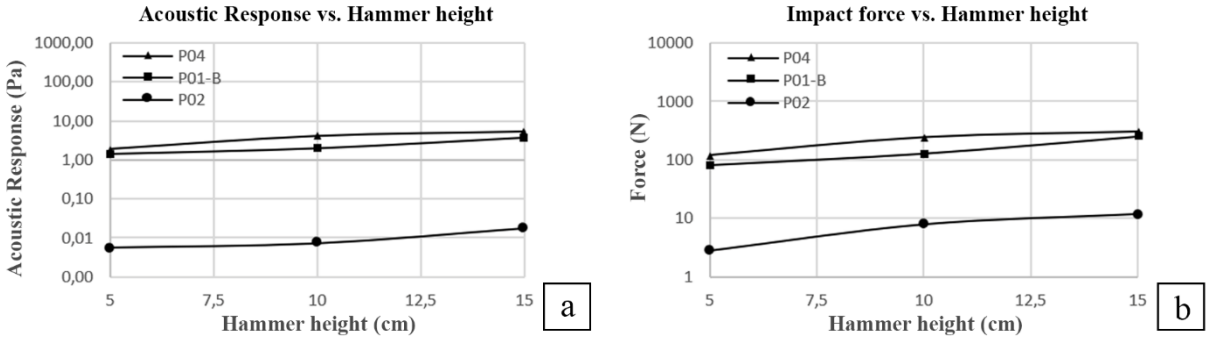

Figure 6. Acoustic response vs. hammer height (a), and impact force vs. hammer height (b)

Conclusions

The aim of this study and the related laboratory tests was to investigate the correlation between mechanical properties and acoustic response of road pavements, through an impact hammer test method.

The following conclusions can be drawn: 1) The standard EN 29052-1 seems to provide a reasonable estimate of resonant frequencies for cylindrical samples, especially in case of rubber. 2) Even if using the hammer test the mechanical impedance and dynamic stiffness can be derived, it should be noted that many parameters could affect the results, due to the complexity of the experimental system, such as sample geometry and under-layer materials. 3) The MDoF system appears to well simulate test configuration. 4) Further investigations are required to have a higher accuracy of the results. This notwithstanding, according to these measurements, the mechanical impedance appears to be a sound indicator to evaluate the acoustic response for frequencies up to 400 Hz.

Funding

This work was supported by the <European Commission> under Grant [LIFE E-VIA 18 ENV/IT/000201].

Author contributions

All the authors conceived the study. Pellicano and Fedele were responsible for data collection and analysis. Praticò was responsible for data interpretation.

Disclosure statement

Authors declare that they have not any competing financial, professional, or personal interests from other parties.

References

American Standard. (1963). *Specifying the mechanical impedance of structures* (USAS S2.6).

ASTM International. (2002). *Standard test method for fundamental transverse, longitudinal, and torsional resonant frequencies of concrete specimens* (ASTM C125).

Bede, N., & Kožar, I. (2016). Determination of dynamic modulus of elasticity of concrete by impact hammer. *HDKBR INFO Magazin*, *6*(1), 8–11.

Bendtsen, H., Andersen, B., Kalman, B., & Cesbron, J. (2013). The first poroelastic test section in PERSUADE. In *42nd International Congress and Exposition on Noise Control Engineering 2013, INTER-NOISE 2013: Noise Control for Quality of Life*, 1, 1–5.

European Committee for Standartization. (2004). *Test methods for hot mix asphalt. Part 26: Stiffness* (EN 12697-26 2004).

European Committee for Standartization. (2004). *Natural stone test methods – Determination of the dynamic modulus of elasticity (by measuring the fundamental resonance frequency)* (EN 14146 2004).

European Committee for Standartization. (1992). *Acoustics – Method for the determination of dynamic stiffness – Part 1: Materials used under floating floors in dwellings* (EN 29052-1 1992).

Fedele, R., Merenda, M., Praticò, F. G., Carotenuto, R., & Della Corte, F. G. (2018). Energy harvesting for IoT road monitoring systems. *Instrumentation Mesure Metrologie*, *17*(4), 605–623. https://doi.org/10.3166/i2m.17.605-623

Harris, C. M., & Piersol, A. G. (2002). *Harris' shock and vibration handbook*.

International Organization for Standartization. (2019). *Mechanical vibration and shock – Experimental determination of mechanical mobility – Part 5: Measurements using impact excitation with an exciter which is not attached to the structure* (ISO 7626-5 2019).

Keulen, W. Van, & Duškov, M. (2005). *Inventory study of basic knowledge on tyre/road noise*. Delft, Netherlands.

Li, M., Molenaar, A. A. A., van de Ven, M. F. C., & van Keulen, W. (2012). Mechanical impedance measurement on thin layer surface with impedance hammer device. *Journal of Testing and Evaluation*, *40*(5), 20120089. https://doi.org/10.1520/JTE20120089

Li, M., Van Keulen, W., Ceylan, H., Cao, D., van de Ven, M., & Molenaar, A. (2016). Pavement stiffness measurements in relation to mechanical impedance. *Construction and Building Materials*, *102*(Part 1), 455–461. https://doi.org/10.1016/j.conbuildmat.2015.10.191

Merenda, M., Praticò, F. G., Fedele, R., Carotenuto, R., & Della Corte, F. G. (2019). A real-time decision platform for the management of structures and infrastructures. *Electronics (Switzerland)*, *8*(10), 1–22. https://doi.org/10.3390/electronics8101180

Morcillo, M. A., Hidalgo, M. E., Pastrana, M. del C., García, D., Torres, J., & Arroyo, M. B. (2019). LIFE SOUNDLESS: New generation of eco-friendly asphalt with recycled materials. *Environments*, *6*(4), 48. https://doi.org/10.3390/environments6040048

Praticò, F. G. (2014). On the dependence of acoustic performance on pavement characteristics. *Transportation Research Part D: Transport and Environment*, *29*, 79–87. https://doi.org/10.1016/j.trd.2014.04.004

Praticò, F. G. (2011). Roads and loudness: A more comprehensive approach. *Road Materials and Pavement Design*, *2*(4), 359–377. https://doi.org/10.1080/14680629.2001.9689908

Praticò, F. G., Ammendola, R., & Moro, A. (2010). Factors affecting the environmental impact of pavement wear. *Transportation Research Part D: Transport and Environment*, *15*(3), 127–133. https://doi.org/10.1016/j.trd.2009.12.002

Praticò, F. G., Fedele, R., & Pellicano, G. (2019). The prediction of road cracks through acoustic signature: Extended Finite Element Modeling and experiments. *ASTM Journal of Testing and Evaluation*, *49*(4). https://doi.org/10.1520/JTE20190209

Radenberg, M., Drewes, B., & Manke, R. (2017). Noise reducing effect of new dense asphalt layers. In *6th Eurasphalt & Eurobitume Congress, (E&E Congress 2016)*, 1–3 June 2016. Prague, Czech. https://doi.org/10.14311/EE.2016.053

Sandberg, U., & Ejsmont, J. A. (2002). *Tyre/road noise reference book*. Kisa, Sweden: Informex.

Siemens. (2019). *Dynamic stiffness, compliance, mobility, and more*. Web site: https://community.sw.siemens.com/s/article/dynamic-stiffness-compliance-mobility-and-more

Skov, R. S. H., Bendtsen, H., Raaberg, J., & Cesbron, J. (2015). *Laboratory measurements on slabs from full scale PERS test sections*.

Vázquez, V. F., & Paje S. E. (2016). Dynamic stiffness assessment of construction materials by the resonant and non-resonant methods. *Journal of Nondestructive Evaluation*, *35*(2), 1–11. https://doi.org/10.1007/s10921-016-0350-z

Vázquez, V. F., & Paje, S. E. (2012). Mechanical impedance and CPX noise of SMA pavements. *Acoustics 2012 Nantes Conference*.

Vázquez, V. F., & Paje, S. E. (2015). Dynamic stiffness assessment of bituminous mixtures type Sma According construction characteristics, (July), 12–16.

WHO Europe. (2011). *Burden of disease from environmental noise: Quantification of healthy life years lost in Europe*. Denmark.